Liquid Crystals
Publication details, including instructions for authors and subscription information:
http://www.informaworld.com/smpp/title~content=t713926090

Fluid self-organized machines

Hans Gruler

Online publication date: 06 August 2010

To cite this Article Gruler, Hans(1998) 'Fluid self-organized machines', Liquid Crystals, 24: 1, 49 — 66
To link to this Article: DOI: 10.1080/026782998207578
URL: http://dx.doi.org/10.1080/026782998207578

LIQUID CRYSTALS, 1998, VOL. 24, NO. 1, 49–66

Fluid self-organized machines

by HANS GRULER
bioPhysics Department, Complex Fluids Group, University of Ulm, D 89069 Ulm, Germany† and Centre d'Ecologie Cellulaire, Hôpital Pitié-Salpétrière, F75651 Paris, Cedex 13, France

Presented at the Capri Symposium in Honour of George W. Gray, FRS held at the Hotel Palatium, Capri, 11–14 *September* 1996

Systems far from thermodynamic equilibrium are discussed, e.g. lasers, amoeboid cells, cell clusters, etc. Different types of instabilities are described by rate equations. The ordered state is produced out of a uniform state and a self-organized machine is obtained. The spatial–temporal pattern of an interfacial instability can be used to build a fluid self-organized automobile (transporter). The temporal pattern makes the machine cycle while the spatial pattern produces the spatial spread machine. The spatial movement of droplets can be directed by using light-sensitive molecules like spiropyran in the interface. The organization of amoeboid cells is discussed. The signal transduction chain of amoeboid migrating cells is approximated; the plasma membrane is the essential element. The membrane contains (i) a detection unit for registering extracellular signals and (ii) a chemical amplifier. The second intracellular signal created performs several functions: (i) the activation of the microfilaments, (ii) the activation of the adhesion proteins and (iii) the renewal of the detection unit. The processes are described by rate equations and the machine equation is extracted. Only the diffusion of the small sized molecules of the second intracellular signal are considered. The theoretical predictions are compared with experimental results: (i) an inactivated cellular state is predicted for low pumping; (ii) an isotropic state for higher pumping (cell adhesion but no migration); (iii) a polar activated cellular state for even higher pumping (adhesion and directed migration); (iv) a bipolar activated cellular state for even higher pumping (cell elongation and orientation). The machine characteristics of the different activated states are discussed: (i) the monopole moment of the loaded receptors is the signal for the speed; (ii) the dipole moment of the receptor distribution in respect to the long axis of the cell is used as feedback signal in the automatic controller responsible for the angle of migration; (iii) the quadrupole moment of the receptor distribution is responsible for cell elongation and orientation. The model predictions are verified for different amoeboid cells, e.g. granulocytes, monocytes, melanocytes, fibroblasts, osteoblasts, neural crest cells, etc. Interacting cells have the ability to form ordered structures. A polar and apolar nematic liquid crystal phase is predicted and actually verified.

1. Introduction

The fabrication of self-organized machines is a promising technique, but unfortunately not well developed [1]. The classical way to make a machine is well known: first, the constructors make a blueprint of the desired machine; then, the craftsmen of the machine-shop build the parts, screw them together and the machine is ready to use. The fabrication of a self-organized machine is in principle very simple. First, special molecules are designed which form by themselves an integral part of the machine structure. Second, all the specially designed molecular components are poured together. Third, the machine organizes itself when the system is connected with an energy source and the machine is ready to use. It is important to realize that the machine is more than the sum of the molecules. Some physical principles for building self-organized machines will be discussed.

The technology of self-organized machines presents advantages compared with classical machines; (i) it is a new nanometer technology since the machine size can have molecular size; (ii) it is a new key-hole technology since the molecules which form the machine can be inserted through a tiny hole; (iii) it is a new repair technology, since molecules which form the machine can be exchanged even when the machine is working.

Self-organized machines do not belong to science fiction since their fabrication is well known in life

†Address for correspondence.

sciences. The following procedure takes place: first, specially designed molecules are produced according to the information written on the DNA. These molecules assemble themselves and form working self-organized machines. Some biological examples will be investigated in respect of the self-organization principles involved.

Self-organized machines can be discussed at different levels, but in all cases ordered structures are created out of a homogeneously distributed state. Different length scales can be considered: (i) *nm-machines*—special macromolecules like enzymes organize themselves for chemical production plants; (ii) *μm-machines*—homogeneous mixtures of different types of molecules like lipids, enzymes, motor proteins, etc. organize themselves to form an ordered structure such as an amoeboid cell; (iii) *cm-machines*—mixtures of different types of cells organize themselves to form an ordered structure like an organ.

First, the formation of coherent light in a laser is discussed as a classical example of self-organization. Second, a fluid self-organized automobile will be built by using an interfacial instability. Third, the self-organization principles of amoeboid cells will be investigated. In the last part, interacting cells are considered which can form liquid crystal states.

2. Energy and entropy

Let us concentrate our discussion on periodic working machines. The starting position of the machine cycle can only be reached if energy is delivered to the machine—the machine has to be connected with an energy reservoir. Thus, a working machine is a system far from thermodynamic equilibrium and energy consumption is one basic feature of periodic working machines. This holds true for classical machines as well as for self-organized machines. In addition the energy consumption of the machine is connected with entropy production which is responsible for process direction, process speed, etc. But the entropy production is also responsible for the creation of ordered structures out of a uniform state.

First, a system like a small sized chemical production plant is considered where only the process direction is determined by the entropy production, but the formation of the system can take place at thermodynamic equilibrium. For example, the cytochrome P-450 dependent mono-oxygenase system consists of the enzyme P-450 and the NADPH-cytochrome P-450 reductase [2]. The protein complex transforms the substrate 7-ethoxy-coumarin, for example, into the product 7-hydroxy-coumarin. The more lipid-soluble substrate is chemically modified to the more water soluble product by using energy which is stored in the NADPH. The so-called preformed complex can be reconstituted *in vitro* from the purified proteins without the energy deliverer, NADPH. The process direction of the enzyme is fully determined by the dissipation process which can be linear.

Now let us consider a non-linear dissipation process where the ordered structure can only exist as long as the dissipation process takes place. A typical example is the spatial–temporal pattern of the chemical oscillatory reactions of Belousov and Zhabotinsky in reference [1]. The entropy production is used not only to describe the direction of all the chemical reactions, but also to create out of the uniform state an ordered structure. If the entropy production is stopped, the ordered structure disappears. Here the spatial–temporal pattern of an amoeboid cell will be discussed. The systems themselves may be physical, chemical or biological, and the result is the spontaneous formation of macroscopic patterns. This self-organization concept is clearly of particular relevance to complex systems, both natural and artificial in origin. It is unfortunate that so little progress has been achieved in the past towards the understanding of synchronization, pattern formation, and turbulence in non-linear, self-oscillatory media and related many-body systems, in spite of their great potential importance. The underlying physics is closely related to the slaving principles whose conceptual importance in non-linear dissipative dynamics in general was emphasized by Haken [1] and first demonstrated by this team in laser theory.

The basic principles for constructing self-organized machines are first discussed in the case of a laser. The entropy production is not considered explicitly, but as the rate equations of quantities of the system which slave the atomic systems. It will be shown that this slaving principle can be used in all the systems discussed.

3. The laser

The laser is nowadays one of the best understood many-body problems. It is a system far from thermal equilibrium and it allows study of cooperative effects in detail. A laser consists of laser-active atoms and a set of two parallel mirrors. If the laser atoms are pumped (excited) only weakly by an external source, it acts as an ordinary lamp; the atoms independently of each other emit wavetracks with random phase. If the pump is further increased, suddenly within a sharp transition region the emitted light of all the laser atoms becomes in phase, though they are excited by the pump completely at random. Thus, the laser atoms show the phenomenon of self-organization. The laser will now be explained to show the similarity to other self-organized systems.

The temporal change of coherent photon number, n, in the laser is a function of the gain and loss. The gain stems from the stimulated emission and is therefore proportional to the number of photons and to the

number of excited atoms, N. The gain of the photon production is then GNn where G is the gain constant. The loss of the photons takes place at one end face (semitransparent mirror) of the laser and is proportional to the number of photons present. The rate equation for the number of coherent photons is then

$$\frac{dn}{dt} = GNn - \kappa n \tag{1}$$

with the loss constant κ. This rate equation becomes non-linear since the number of excited atoms decreases with the emission of photons. Without the laser action, the number of excited atoms is a fixed number, N_0, produced by the pump. The actual number of excited atoms will be reduced due to the laser process, because the coherent photons constantly force the atoms to return to their ground state (α characterizes this process)

$$N = N_0 - \alpha n. \tag{2}$$

The rate equation for the laser photons is now

$$\frac{dn}{dt} = (GN_0 - \kappa)n - \alpha G n^2. \tag{3}$$

No coherent light is emitted for small pumping, where N_0 is small and $GN_0 - \kappa < 0$. The laser emits coherent light for strong pumping, where N_0 is large and $GN_0 - \kappa > 0$. The number of coherent photons or the electric field amplitude of the laser light can be regarded as the essential order parameter, since the excited atoms are slaved by this order parameter to emit stimulated light.

The laser was shown as an example of self-organization; the same principles may be applied to build a self-organized automobile.

4. Fluid self-organized automobile

We are interested in building a fluid self-organized automobile. The task will be solved in two steps: first, the coherent movement of atoms is produced by an interfacial instability and second, the instability is steered by a weak external signal.

The following system is considered (figure 1): two liquids such as an aqueous liquid and an organic solvent are poured together. The immiscible liquids form two distinct phases even at thermodynamic equilibrium. The system is moved far from thermodynamic equilibrium by dissolving (i) a surface active hydrophobic material in the aqueous liquid and (ii) a hydrophilic material in the organic solvent. Diffusion currents through the interface occur since each compound is dissolved in the phase where it is less soluble. During the diffusion process, the hydrophilic and the hydrophobic molecules are pumped into the interface where they form a metastable complex with a certain lifetime. The important fact is that the metastable complex lowers the surface tension of the interface; no instability is observed if only one compound is pumped to the interface.

For small pumping, the interface is flat and the movement of the molecules in the interface is random. But for a large pumping, the interface is undulated and the molecules of the interface make a coherent movement even when the pumping is random. Thus, the order parameter of the interfacial instability is the amplitude, C, of the undulations.

The temporal change of the undulated interface is a function of gain and loss. The gain stems from the stimulated undulation and should be proportional to the density, N, of the 'excited' molecules pumped to the interface, and to the undulation amplitude, C. The gain is GNC where G is the gain constant. The rate equation for the undulation amplitude is (gravitational effects are neglected)

$$\frac{dC}{dt} = GNC - \kappa C \tag{4}$$

with the loss constant κ. In the case of no pumping ($N = 0$), the undulation amplitude approaches exponentially the flat state with the characteristic time κ^{-1}. This rate equation becomes non-linear since the density, N, decreases with the undulation of the interface. There is on the one hand the dilution effect by the surface increase, but on the other hand the dissolving of the interfacial complex and the flow of the molecules to the desired liquid. It is assumed that the density of the 'excited' molecules projected on a flat interface is a fixed number, N_0, produced by the pumping. One has the following relation

$$N = N_0 - \alpha C. \tag{5}$$

The rate equation for the undulation amplitude is then

$$\frac{dC}{dt} = (GN_0 - \kappa)C - \alpha G C^2. \tag{6}$$

A flat surface is expected for small pumping (small N_0) since the surface tension, σ, is positive ($\sigma \propto \kappa - GN_0 > 0$) and the molecules in the interface perform random movements. An undulated interface is expected for large pumping (large N_0) since the surface tension, $\sigma (\propto \kappa - GN_0 < 0)$ is negative and the molecules of the interface make correlated movements. Note that not all molecular details responsible for the interfacial instability are known, but the similarity to the laser is evident: the coherent interfacial wave acts in a similar way to the coherent light wave in a laser.

A surface instability is observed by using the following types of compound and solvents [3, 4]: (i) hydrophilic materials like picric acid or potassium iodide are dissolved in an organic liquid like nitrobenzene or

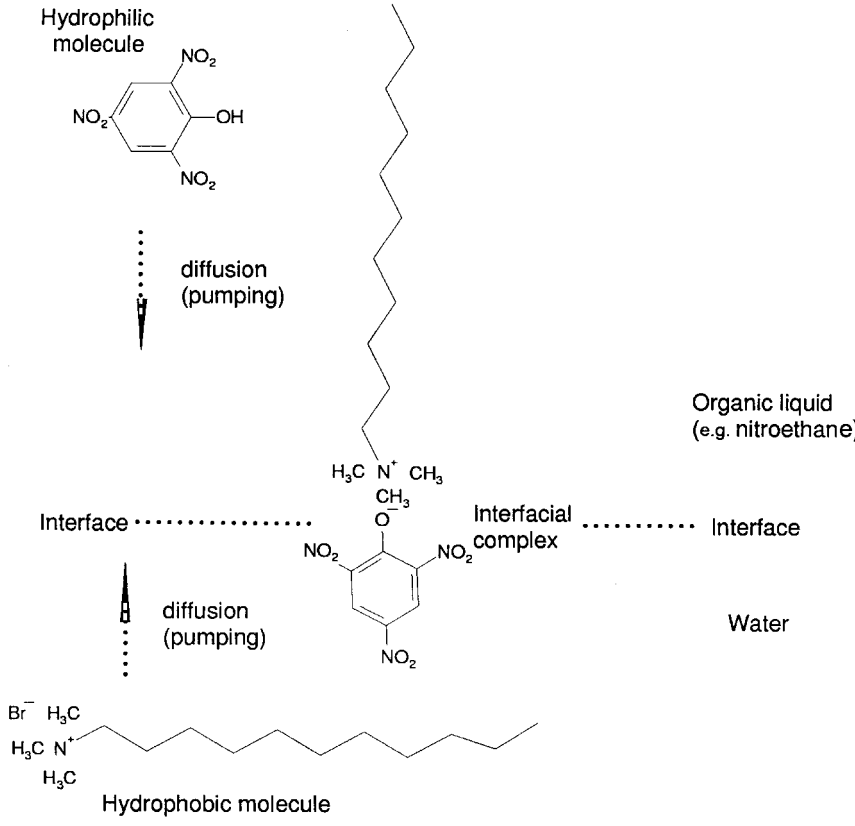

Figure 1. Schematic representation of the interfacial system. The hydrophilic compound diffuses from the organic liquid through the interface to the water phase where it is more soluble; the hydrophobic compound diffuses in the opposite direction. The hydrophobic and the hydrophilic compounds form at the interface a metastable complex which lowers the interfacial tension.

nitroethane; (ii) hydrophobic molecules such as long chain alkyltrimethylammonium halides are dissolved in water. The chosen molecules form a long living complex at the interface which lowers the interfacial tension. Emulsification is suppressed by choosing the molecules in such a way that the interfacial complex creates a small spontaneous curvature. The liquids are poured together in a glass cup (8 cm in diameter). At the beginning, the interface is flat and quiet, then after a few minutes the interface becomes disturbed. Quasi-periodic interfacial waves with small amplitudes and large wave numbers are observed. The final state is a single surface wave with 1–2 cm height moving clockwise or anticlockwise. The surface waves are observed as long as the pumping of both types of molecule is strong enough; no instability is observed if only one type of molecule is strongly pumped.

Next, the construction of a fluid self-organized automobile by means of this interfacial instability will be described. One liquid phase is reduced to a drop which is surrounded by the other liquid. This drop of several millimetres in diameter is put on a glass surface or allowed to float in a density gradient of the other liquid (figure 2). For large diffusion currents the instability

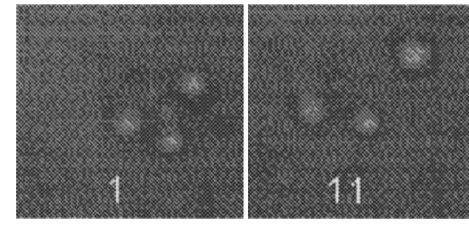

Figure 2. Drops of nitroethane containing $1{\cdot}25 \times 10^{-3}$ M picric acid are surrounded by water containing 5×10^{-3} M dodecyltrimethylammonium bromide ($C_{12}Br$). The drops are floating on a sugar density gradient; they have a diameter of about 1·5 mm. The time difference between the two pictures is about 1 min.

starts at one point of the interface and moves towards the opposing pole. During this process a net impetus is created, the drop is caused to move and a kicking motion of the whole drop is observed. The speed of the motion slows down due to friction, and it takes about 1 min before the next cycle of instability can start. The observations can be characterized as a spatial–temporal pattern of the interfacial instability: the temporal pattern defines the machine cycle and its characteristic time is

given by a diffusion controlled process. The spatial pattern defines the motor characteristic.

In an isotropic environment, the orientation of the spatial pattern (motor characteristic) is isotropic and the drops perform random walk. The analogy to Brownian motion is evident, but there is a big difference since the drop makes an active movement, whereas the irregular movement of a small colloidal particle is caused by impacts with molecules of the liquid. In short the Brownian particle is moved by thermal energy. If the movement of the drop were produced by thermal motion, then the calculated temperature would be 10^{10} K. This quasi-temperature would need to be high since the large sized drop moves within 1 min a distance of its size. This calculated temperature has no physical meaning, it simply demonstrates that the motion of the drop is produced by an active process.

It is desirable to control the motion of the drop by a weak external signal. This task is solved by introducing molecules in the interface which can alter the interfacial tension as a function of an external signal. A copolymer is used: it contains a chromophore (spiropyran) which alters the surface tension under the influence of light (figure 3). UV opens one ring in the spiropyran molecule and a large electric dipole is created which decreases the surface tension of the interface [5]. This molecular modification is stable even when the light is switched off. The effect is reversible since the original molecular modification is obtained by absorption of visible light. The backbone of the copolymer is chosen in such a way that the whole molecule is trapped in the interface.

The onset of the instability can be influenced by the chromophores since one expects an increase in the decay time, κ^{-1}, if the surface tension is lowered and, thus, the threshold condition for the instability is lowered. This means that the UV-illuminated part of the interface is the start of the interfacial wave. Or in other words, the orientation of the spatial pattern of the interfacial instability can be influenced by a weak external signal. Thus, the fluid self-organized automobile can be steered by a weak external signal.

The active movement of a drop can be conducted by light, but such a system has no real application since the stored energy is very small. Only a small number of cycles can be observed and then the active migration stops. Thus, the active movement of the drop is interesting only from a scientific point of view. To learn more about self-organized fluid machines one has to go to biological systems. We come now to the field of biologically inspired physics; a few examples are shown.

5. Self-organization of amoeboid cells

It is hard for a physicist to work in the field of cell biology, but one can learn to handle cells by cooperating with cell biologists. Our investigations are basically performed with human granulocytes (figure 4) which form in mammalians the first defense line against invading micro-organisms. These cells migrate on a substrate like an amoeba by changing their shape. It is important to realize that the basic biochemical reactions of the cellular signal transduction chain are known [6]. Besides granulocytes, other cell types have been investigated, e.g. monocytes, lymphocytes, melanocytes, fibroblasts, osteoblasts and neural crest cells, to name a few. All cells investigated migrate like an amoeba.

A granulocyte contains many different machines since it has the ability to handle different kinds of situations, but here we are only interested in the

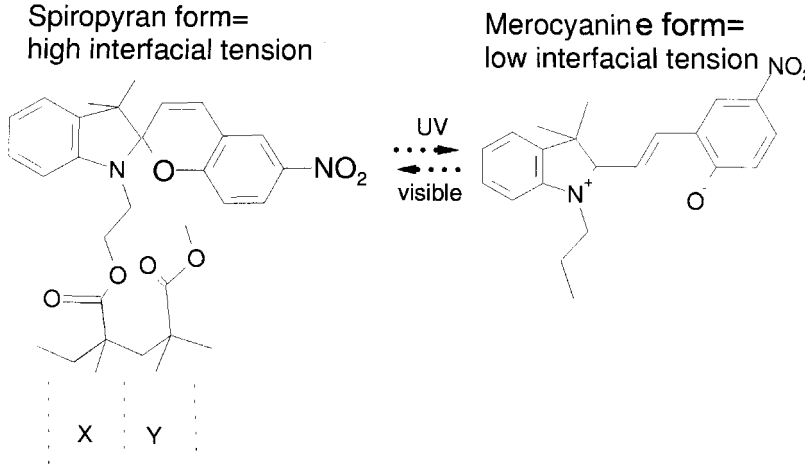

Figure 3. Photochromic indolinospiropyran groups (5 mol %) are covalently attached to a polymer backbone of poly(methy methacrylate). Ultraviolet light excitation (365 nm) induces a heterolytic cleavage of the closed spiropyran structure. The zwitterionic merocyanine structure lowers the interfacial tension. The highly conjugated merocyanine form absorbs light in the visible (520–560 nm) and the original spiropyran form is obtained.

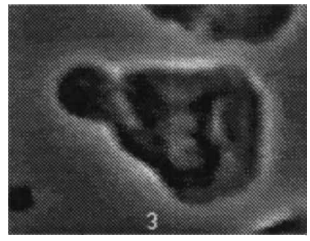

Figure 4. A human granulocyte stimulated by blood plasma is migrating on a glass slide. The cell is migrating to the right side; the front part is the leading front (motor). The cell length is about 20 μm.

machinery responsible for migration. Therefore, one would like to investigate the isolated motile apparatus of a cell as a model of fluid self-organized machines. Keller and Bessis [7] discovered a self-purification of the motile machinery some time ago in granulocytes subjected to a carefully controlled and timed application of heat. This treatment causes the leading edge (motor) of the cell to move forward rapidly, forming a long thin stalk of cytoplasm that often breaks to form two separate units, the cytokineplast and the cell body (figure 5). The machinery which creates the cell locomotion contains only a few elements: a part of the plasma membrane, unstructured cytoplasm as seen by the light microscope, and the necessary biochemistry. Most important, the newly formed cytokineplasts are capable of membrane movement, including adherence, spreading, random locomotion, directed migration, and phagocytosis [8].

A cytokineplast is just a membrane enclosing the appropriate chemistry. The important cellular elements are: (i) the *detection unit* creating out of the extracellular signal the so-called first intracellular signal; (ii) the *chemical amplifier* creating out of the first intracellular signal the so-called second intracellular signal; (iii) the *reaction unit* acting according to the second intracellular signal. The order parameter which slaves the cellular chemical reaction is the second intracellular signal. A schematic representation of the cellular signal chain is shown in figure 6.

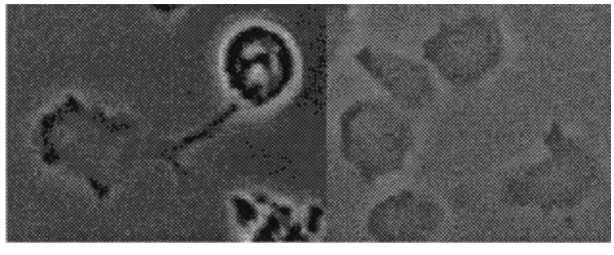

Figure 5. The cellular motor of a human granulocyte moved out of the cell. The motor (cytokineplast) is connected with the cell body by a thin stalk (left side). The cytokineplasts alone are seen in the right side; their characteristic length is about 5 μm.

The action of a cell can be compared with a laser and an interfacial instability. For weak pumping, the action of the muscle proteins is random and 'no' cellular action is expected (=inactivated cellular state). But for strong pumping, the action of the muscle proteins is coherent even when the pumping is random and a coherent cellular action is expected (=activated cellular state).

In the next step, the essential rate equations for the self-organization in the cellular signal chain are derived.

5.1. *Detection unit*

One main function of the plasma membrane is to separate the intracellular space from the extracellular space. In addition to this main function, the membrane is also the first element in the signal transduction chain.

The first step in the signal chain of the cellular machine is the provision of new receptors in the plasma membrane (concentration R).

$$\frac{\mathrm{d}R}{\mathrm{d}t} = F(M) - k_{1e}R - k_{11}Rc + k_{22}R_C. \tag{7}$$

The provision of new receptors is described by $F(M)$. A vesicle fusion process is assumed. The vesicle fusion is induced by the signal molecules coming out of the chemical amplification chain, the second intracellular messengers (concentration M). The second term describes the deactivation of the receptors. The last two terms describe the binding kinetics between the kinesis stimulating molecule (concentration c) and the receptor. The rate equation for the loaded receptors (concentration R_C) is

$$\frac{\mathrm{d}R_C}{\mathrm{d}t} = k_{11}Rc - k_{22}R_C - k_{2e}R_C. \tag{8}$$

The first two terms describe the binding dynamics of the kinesis stimulating molecules to the receptors. The inactivation of the occupied receptors is described by the third term.

An adiabatic approximation can be used since the receptor loading kinetics are fast compared with the temporal variations of the receptor density. The steady state concentrations of the first intracellular signal, R_C^{st}, is ($k_{1e} + k_{2e} \ll k_{11}$)

$$R_C^{st}(t) = \frac{1}{k_{1e} + k_{2e}} \frac{c}{c + K_R} F(M) \tag{9}$$

with the equilibrium constant, $K_R = k_{22}/k_{11}$. The first intracellular signal—the receptor density of the activated receptors, R_C^{st}—is as expected the product of (i) the receptor supply function, $F(M)$, (ii) the fraction of loaded receptors, $c/(c + K_R)$, and (iii) the lifetime of the activated receptors, $\tau = 1/(k_{1e} + k_{2e})$.

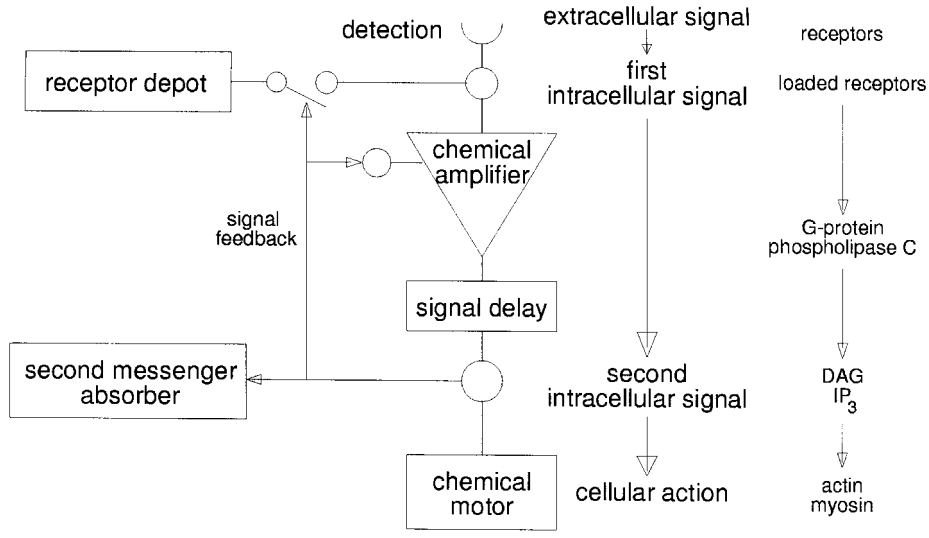

Figure 6. Schematic representation of the cellular machine. The middle part shows the phenomenological description of the cellular signal transduction/response system. The left part of the figure shows a physical description of the cellular signal transduction/response system where functional units are used in the information flux diagram. The right part shows the important cellular molecules involved.

5.2. *Chemical amplifier*

The activated receptors are the first element in the biochemical amplification chain: (i) one loaded receptor activates many membrane-attached G-proteins; (ii) one G-protein activates the membrane-bound phospholipase-C protein; (iii) one phospholipase-C protein hydrolyses many ATP-activated phospholipid (phosphatidylinositol) molecules of the inner side of the membrane. The water soluble head group, inositol triphosphate (IP_3) and the remaining lipid, diacylglycerol (DAG) belong to the family of second intracellular signal molecules.

The first intracellular signal, R_C, activates the chemical amplification chain. The signal, $S_N(t)$, coming out of the amplification chain has the following form [9]

$$S_N(t) = \frac{f_0^{N-1}}{(N-1)!}\int_0^t t'^{N-1} \times \exp[-f_0 t']R_C[M(t-t')]B(M)\,dt'. \quad (10)$$

It is assumed that the amplifier contains N steps with equal forward rate constants f_0. The output signal of the amplification chain, S_N, is a function of the input signal $R_C[M(t-t')]$ at previous times $t-t'$. In addition, it is assumed that the amplifier characteristics, $B(M)$, depends on the second intracellular signal. The sharp input signal is broadened by the chemical reactions and one obtains a Poisson distributed output signal.

The chemical amplifier can be characterized either by the number of rate equations, N, or the lagtime, T $(=N/f_0)$, between the input and the output signal. The proposed lagtime can be determined by field-jump experiments. A guiding field, such as a concentration gradient of kinesis stimulating molecules or an electric field, is applied and the cellular response is measured. For example, the observed lagtime between the change in the electric field and the first cellular reaction of granulocytes was 8–10 s [10, 11]; concentration gradient jump experiments lead to similar values [9, 12].

5.3. *Second intracellular signal*

The temporal change of the second intracellular messenger depends on the gain, G, and the loss H

$$\frac{dM(t)}{dt} = G[M(t-t')] - H[M(t)]. \quad (11)$$

The cellular signal chain supplies the second intracellular signal with fresh molecules. One can say that the cellular signal chain acts as a pump. The gain—the output of the chemical amplifier—is a function of (i) the receptor supply function, $F(M)$, (ii) the fraction of occupied receptors, $c/(c+K_R)$, (iii) the lifetime of the activated receptors, τ, and (iv) the amplifier characteristics, $B(M)$. The receptor supply, $F(M)$, the amplifier characteristics, $B(M)$, and the loss, $H(M)$, are functions of the second intracellular signal.

The temporal feature of the cellular signal transduction chain is described by this differential equation (11), but the spatial variations of the signal chain are not yet considered. The second intracellular signal is a function not only of the time, but also of the space. The spatial features in the signal chain can be introduced in the following way. We consider two neighbouring area elements of the membrane at the position x and $x+\Delta x$

(figure 7) with the cell fixed coordinate system x; for simplicity, only one coordinate is considered. The concentration of the first intracellular signals in these two area elements is $R_C(x)$ and $R_C(x+\Delta x)$. The diffusion of the first intracellular signal molecules is neglected since the membrane-bound receptors have a large size (high molecular mass) and, thus, the diffusion process is slow. The same argument holds for the chemical amplification chain. The proteins involved like G-protein and phospholipase C are large, and therefore the slow diffusion process can be neglected. But diffusion of the second intracellular molecules cannot be neglected since the signal molecules such as the membrane-bound lipid diacylglycerol (DAG) and the water soluble ion inositol triphosphate (IP_3), are small (low molecular mass) and, therefore, the diffusion is high. The rate equation for the second messenger is

$$\frac{\partial M(x, y, t)}{\partial t} = G[M(x, y, t-t')] - H[M(x, y, t)] + D\Delta M(x, y, t) \qquad (12)$$

with the lateral diffusion coefficient, D, for the second intracellular messenger molecules and the Laplace operator $\Delta = (\partial^2/\partial x^2 + \partial^2/\partial y^2)$. In the present model no distinction is made between the different second intracellular messenger molecules.

The order parameter of the self-organized machine is the second intracellular signal which slaves many cellular chemical reactions such as the receptor supply, the chemical amplifier, the chemical motor, the adhesion process, etc. Thus, the cellular action can be predicted if the behaviour of the second intracellular signal is known. A detailed prediction can be made by solving

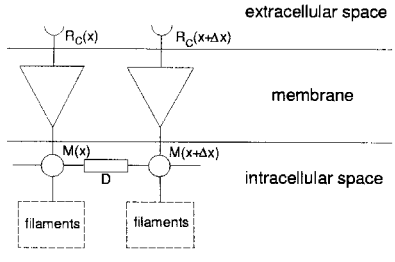

Figure 7. Schematic representation of an active membrane. The first cellular signal, R_C, exists in the form of membrane-bound receptors loaded with chemicals of the extracellular space; this signal is chemically amplified and the second intracellular signal, M, is obtained. The amplifier works with membrane-bound and membrane-attached proteins; the second intracellular signal is localized in the membrane or very close to it. Two membrane elements are shown at the positions x and $x+\Delta x$. It is assumed that there exists only a lateral diffusion of the second intracellular signal molecules. One of the functions of the second intracellular messenger molecules is the activation of filaments.

equation (12). Note that the rate equations for describing the laser, the interfacial instability, and the amoeboid migrating cell, have a similar structure.

5.4. *Instability of the second intracellular signal*

Next, the spatial–temporal instability of the cellular signal chain will be discussed. A part of the calculations is already published [9]. First, the steady state value, M_0, of the second messenger is determined where the gain equals the loss; $G(M_0) - H(M_0) = 0$. The steady state value, M_0, increases monotonically with the concentration, c, of the kinesis stimulating molecule.

The onset of the instability can be determined if the system close to M_0 is investigated; thus, a Taylor series of the gain and the loss function are made. In the subsequent equations, the abbreviation, $m = M - M_0$, and the dimensionless time, $t^* = f_0 t$, are used.

$$f_0 \frac{\partial m}{\partial t^*} = G_0' m(t^* - N) - H_0' m(t^*) + D\Delta m \qquad (13)$$

with

$$G_0' = \left.\frac{\mathrm{d}G}{\mathrm{d}m}\right|_{M_0} \qquad (14)$$

$$H_0' = \left.\frac{\mathrm{d}H}{\mathrm{d}m}\right|_{M_0}. \qquad (15)$$

This partial differential equation can be solved by a separation ansatz (the solution is shown only for one dimension)

$$m(t^*, x) = \Theta(x) \exp(\tilde{\lambda} t^*). \qquad (16)$$

One obtains the following eigenvalue equation for the spatial distribution of the second intracellular messengers at the plasma membrane.

$$\frac{\mathrm{d}^2\Theta}{\mathrm{d}x^2} + \frac{A(\tilde{\lambda})}{D}\Theta = 0 \qquad (17)$$

$$A(\tilde{\lambda}) = G_0' \exp(-\tilde{\lambda} N) - H_0' - f_0\tilde{\lambda}. \qquad (18)$$

The unknown spatial distribution function, $\Theta(x)$, in the separation ansatz can be expressed by a Fourier series as the problem is periodic with 2π

$$\Theta(x) = \sum_{n=-\infty}^{\infty} c_n \exp(\mathrm{i}K_n x). \qquad (19)$$

It is assumed that the plasma membrane can be approximated by the surface of a cylinder with the circumference, L. The wave vector has the following form

$$K_n = \frac{2\pi n}{L} \qquad (20)$$

where n is an integer. The temporal behaviour of the cellular signal chain is described by $\lambda(= f_0\tilde{\lambda})$. It is a

complex number which can be split into its real and imaginary parts, $(\mu + i\omega)$. For $\mu < 0$, temporal oscillations in the cellular signal chain are damped, and thus the system reaches a stable state. But for $\mu > 0$, the amplitude of the oscillations increases with time. Thus, a critical condition is reached if the real part vanishes, $\mu = 0$.

5.4.1. *Temporal pattern*

First, the temporal pattern of the instability will be discussed. The oscillation frequency, ω, which characterizes the temporal pattern is closely related to the delay time, T, in the signal-response system. At the threshold, ω is $\approx 1{\cdot}67\pi/T$ and approaches $1{\cdot}67\pi/T$ for large G_0'. Thus, the delay time of the signal chain is expected to be slightly smaller than the characteristic time, T_{osc}, of the oscillations ($T/T_{osc} \leqslant 0{\cdot}835$). This prediction is verified by experiments.

Some experiments which demonstrate the predicted temporal oscillations in the cellular signal chain are described. (i) The electric membrane potential difference, $U(t)$, can be measured by means of micro-electrodes as a function of time. Molecules of the family of the second intracellular cellular signal chain can activate ion channels of the plasma membrane and the electric membrane potential difference, $U(t)$, will alter its value due to the ion flow through the channel. Thus, a periodic fluctuating electric membrane potential difference, $U(t) = U(t + T_{osc})$, is expected. The measured repetition of the membrane potential difference is 8 s [13]; the measured repetition time is approximately the measured delay time as predicted by the model. (ii) The intracellular calcium concentration is discussed as an important intracellular signal and, hence, one expects periodic oscillations in the intracellular calcium concentration. But, up to now, we have not successfully shown fluctuations of the calcium concentration with a characteristic time of 8 s in granulocytes [14]. But cytokineplasts, after stimulation with the chemoattractant Leukotriene B_4, show a transient increase in the intracellular calcium concentration and damped periodic oscillation with a repetition time of 8 s [15]. (iii) The filaments (f-actin) are one basic element of the amoeboid motor. One expects that the second intracellular messengers can affect the production of the filaments; therefore, one expects periodic oscillations of the filament concentration. The total cellular amount of f-actin filaments was measured in granulocytes and one finds small variations with a characteristic time of 8 s [16]. (iv) One expects rhythmic shape changes if the periodic second intracellular signal activates the cellular motor proteins. As expected, rhythmic shape changes are found with a periodicity of 8 s for suspended granulocytes [16]. (v) It is well known that periodic external signals can synchronize self-oscillatory media, therefore, one expects that the intrinsic oscillation of the cellular signal chain can be influenced by periodic extracellular signals. As expected, granulocytes can be synchronized by short electric field pulses with a repetition time of a multiple of 8 s [17].

The temporal oscillation of the cellular signal transduction/response system is very well verified for granulocytes and in accordance with the model predictions: the measured delay time in the signal is approximately the characteristic time of the oscillations, as predicted. This is strong evidence that the model describes basic features of the self organized machine even when not all the details of the signal chain are known.

5.4.2. *Spatial pattern*

Next, the spatial pattern of the cellular signal chain will be discussed. The spatial pattern of the instability is characterized by the wave vector, K_n. The instability occurs for $G_0'^2 - \omega^2 - (H_0' + DK_n^2)^2 > 0$. Different spatial modes, K_0, K_1, K_2, etc. of activated cells are possible. They can be obtained for different concentrations, c, of the kinesis-stimulating molecules (constant temperature) or different temperatures, T (constant concentration c), since the gain, G, of the signal chain depends on the concentration and on the temperature (figure 8). Note, only some principles of the instability are discussed but no details are given.

5.4.2.1. *Inactivated cellular state.* No coherent spatial–temporal pattern in the cellular signal chain is expected for small concentrations ($c < c_0$) or low temperature ($T < T_0$). The pumping of the cellular signal chain is weak, G_0' is small and $G_0'^2 - \omega^2 - H_0'^2 < 0$. The cell is in a chemokinetic inactive state where the muscle proteins act incoherently. No cellular actions are expected, i.e. no or very weak adherence to a substrate, and no cellular motor (leading front).

5.4.2.2. *Activated cellular states.* A coherent spatial–temporal pattern in the cellular signal chain is expected for either large enough concentrations ($c > c_0$) of the chemokinetic extracellular stimulus or higher temperature ($T > T_0$). The active and the inactive cellular state are separated by the threshold concentration, c_0, of the chemokinetic stimuli or the threshold temperature, T_0. The pumping of the cellular signal chain is strong and G_0' is large; $G_0'^2 - \omega^2 - (H_0' + DK_n^2)^2 > 0$ and a spatial–temporal pattern in the cellular signal chain is expected. The signal molecules as well as the muscle proteins act in phase even when the pumping is random. Cellular actions are expected, i.e. strong adherence to a substrate, and a cellular motor (leading front).

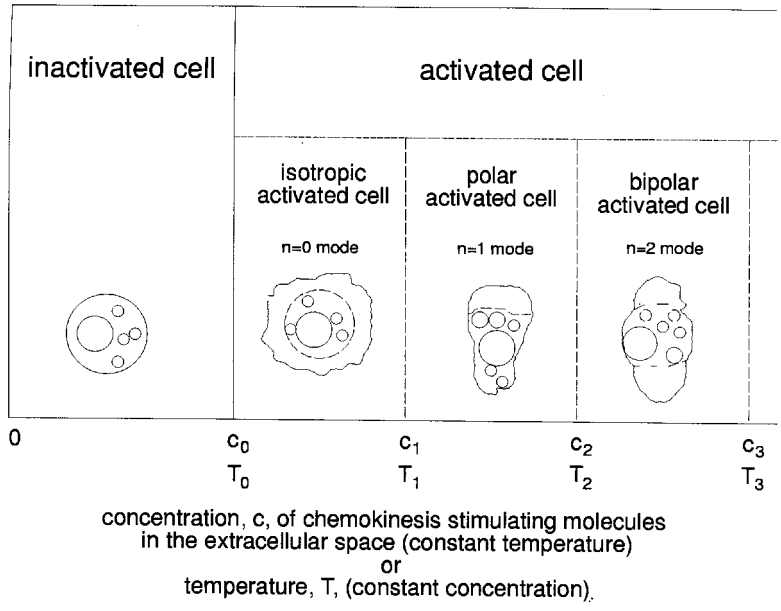

Figure 8. Schematic representation of different cellular states. The activated cell can be in different modes: isotropic mode ($n=0$), polar mode ($n=1$), bipolar mode ($n=2$), etc. The pumping of the cellular signal chain can be altered by (i) the concentration, c, of the kinesis stimulated molecules in the extracellular space (at constant temperature) or (ii) the temperature, T, (at constant concentration).

Isotropic mode. Temporal oscillations with isotropic spatial distribution ($K_0, n=0$ mode) of the cellular signal molecules are expected in the concentration range $c_0 < c < c_1$, or in the temperature range $T_0 < T < T_1$. The pumping of the cellular signal chain is strong enough to create the isotropic mode ($K_0, n=0$ mode), since $G_0'^2 - \omega^2 - H_0'^2 > 0$, but too weak for creating the polar mode ($K_1, n=1$ mode), since $G_0'^2 - \omega^2 - (H_0' + DK_1^2)^2 < 0$. The signal molecules, as well as the muscle proteins act in phase, but no direction is preferred. One expects: (i) an isotropic distribution of the leading front around the cell body and (ii) strong adherence to the substrate. The isotropic mode is actually observed for many cell types.

Polar mode. Beside an isotropic active state a polar active state can occur in the concentration range $c_1 < c < c_2$, or temperature range $T_1 < T < T_2$, where the signal molecules are polar in distribution ($K_1, n=1$ mode). The pumping of the cellular signal chain is strong enough to create the polar mode ($K_1, n=1$ mode) since $G_0'^2 - \omega^2 - (H_0' + DK_1^2)^2 > 0$, but too weak for creating the bipolar mode ($K_2, n=2$ mode), since $G_0'^2 - \omega^2 - (H_0' + DK_2^2)^2 < 0$. The signal molecules, as well as the muscle proteins act in phase in a preferred direction. One expects (i) a polar shaped cell, (ii) a leading front pointing in one direction, (iii) a cell migrating in the direction of the leading front. In addition, the orientation of the polar mode of the cellular signal chain can be influenced by a weak extracellular signal resulting in directed migration as observed for many cell types.

Bipolar mode. Beside the isotropic and polar active states a bipolar active state can occur in the concentration range $c_2 < c < c_3$, or the temperature range $T_2 < T < T_3$, where the signal molecules are bipolar in distribution ($K_2, n=2$ mode). The pumping of the cellular signal chain is strong enough to create a bipolar state since $G_0'^2 - \omega^2 - (H_0' + DK_2^2)^2 > 0$, but too weak for creating an octopolar mode ($K_3, n=3$ mode), since $G_0'^2 - \omega^2 - (H_0' + DK_3^2)^2 < 0$. The signal molecules, as well as the muscle proteins act in phase in two opposing directions. One expects: (i) a bipolar shaped cell, (ii) two separated leading fronts pointing in opposing directions, (iii) cell elongation in the direction of the two opposing leading fronts. In addition, the orientation of the bipolar mode of the cellular signal chain can be influenced by a weak external signal, resulting in cell alignment as observed for many cell types.

Further excited cellular states ($n>2$) are possible and observed but not very well investigated.

5.5. *Experimental observations*

Next, some experiments are discussed which show the predicted cellular states.

5.5.1. *Inactivated cellular state*

An inactive cellular state is expected for low temperature or low concentration of kinesis stimulating

molecules. (i) The inactivated state of cells like granulocytes or monocytes is observed in a kinesis stimulating solution, e.g. blood plasma, and at low temperature, e.g. 4°C. The cells are more or less spherical, do not adhere at the substrate, and show no leading front and no migration. (ii) The inactivated state of cells like granulocytes or monocytes is observed at high temperature, e.g. 37°C, and with no kinesis stimulating molecules in the solution; cells were washed in HBSS (Hank's balanced salt solution) which keeps the cell alive, but does not contain kinesis stimulating molecules. But, there is a problem with granulocytes. They show the predicted behaviour only for a small time period. If one waits, e.g. half an hour, then a large fraction (50%) of the cells migrate on the glass slide even in a medium free of kinesis stimulating molecules; the cells obviously have the ability of self-stimulation. This point plays a fundamental role in the cell–cell communication which will be discussed at the end of this article.

5.5.2. *Isotropic activated cellular state*

An isotropic activated cellular state is expected at higher temperature or higher concentration of kinesis stimulating molecules. The cells are more or less spherical, surrounded by an actively moving leading front and adhered to the substrate. This adherence process is frequently described as a function of temperature or concentration of kinesis stimulating molecules. An isotropic activated cellular state is obtained if a small amount of kinesis stimulating molecules is added—for example monocytes in HBSS diluted blood plasma. Adhering spherical cells are observed which are surrounded by an actively moving veil. One has the characteristic cellular features as predicted for an activated cell in the $n=0$; this state can easily be observed on monocytes (see later in figure 11) but it is less pronounced on granulocytes.

5.5.3. *Polar activated cellular state*

The polar activated state is easy to obtain with granulocytes (figure 4). The general observation is that the leading front is located at one side of the cell and the cellular shape becomes polar even in an isotropic environment. The leading front acting as the cellular motor pulls, and the whole cell moves. A cell in the polar activated state shows a leading front in one direction and gives the cell a polar appearance: at one side the leading front and at the other side the cell body. The leading front exhibits active movement; in addition, the leading front produces a net force which drags the whole cell. Directed migration is possible since the direction of the force produced can be altered by an extracellular signal. One has the characteristic cellular features as predicted for an activated cell in the $n=1$ mode.

The polar active state is observed in many different amoeboid cells such as granulocytes, monocytes, mast cells, single slime mould cells, etc. Less pronounced is the polar active state of fibroblasts, osteoblasts, neural crest cells, etc. Note, not only migrating but also growing cells can be characterized by a polar activated state. Typical examples are the nerve cones of growing dendrites, the dips of growing hyphen (roots), the dips of growing rhizoids (roots), etc.

5.5.4. *Bipolar activated cellular state*

A bipolar activated state is not observed in granulocytes and monocytes, but melanocytes (the pigment cells of the skin) show a very nice bipolar cellular state (figure 12). First the cell is spherical, then two opposing dendrites start to grow. A cell in the bipolar activated state shows two opposing leading fronts and gives the cell a bipolar appearance: the cell body is in the middle and on both sides are leading fronts. The leading fronts exhibit active movement; in addition each leading front produces a net force which elongates the whole cell, but without a mean displacement. Cell orientation is possible, since the sign of the torque produced by the two leading fronts, can be altered by an extracellular signal. One has the characteristic cellular features as predicted for an activated cell in the $n=2$ mode.

The bipolar active state is observed in different amoeboid cells such as melanocytes, fibroblasts, osteoblasts, neural crest cells, slime mould cells, etc. Not only elongation and orientation, but also growth can be characterized by a bipolar activated state, e.g. hair roots where two opposing roots grow out of the main root. A cytokineplast can also create a bipolar state; the following experiment is performed. A cytokineplast is forced to crawl into a narrow glass tube. At the start of the experiment, the cytokineplast has one leading front in one direction—the forward direction. But one observes within several minutes a diminishing of the speed until the cytokineplast stops, since the cytokineplast creates on both sides of the cylinder a leading front. The cell stops if the motors on both ends have reached the same strength. Such a switch has not yet been observed for the whole cell; obviously the leading front on one side is stabilized by the cell body. Such a stabilizing element is missing in cytokineplasts.

Higher order modes are observed but have not been very well investigated.

5.6. *Cellular machinery*

The plasma membrane is an important cellular compartment for cell migration. The signal chain starts with the activated membrane-bound receptors as the first

intracellular signal; the second intracellular messengers are produced and located in and close to the plasma membrane. One action of the second intracellular signal is the provision of the membrane with fresh receptors by vesicle fusion. An essential role is played by the phospholipid (phosphatidylinositol) of the inner side of the membrane. The bulky head group of the ATP-activated phospholipid prevents vesicle fusion due to its positive spontaneous curvature. But then, after action of the phospholipase-C protein, the remaining lipid diacylglycerol (DAG) induces a negative spontaneous curvature which encourages vesicle fusion.

Another cellular action is connected with the cellular signal chain. The f-actin filaments are elongated at the side of the plasma membrane and shortened at the other end. A gel is formed by cross-linking the flexible filaments with myosin. One expects a mean polar orientation at least close to the membrane, but up to now no birefringence has been detected.

Cells like granulocytes make an adhesion with the substrate every 8 s. The adhesive membrane can be visualized by superposing several pictures of a migrating cell; the adhering membrane shows no fluctuations, but the non-adhering membrane does. The distance between the adherence points in the direction of migration is several μm in the case of granulocytes. The speed calculated from the distance between the adhering points and the characteristic time of the cellular signal chain is $22 \pm 3\,\mu m\,min^{-1}$; the measured speed of the whole cell is $22 \pm 4\,\mu m\,min^{-1}$. The cellular linear motor obviously moves with a constant speed, but this picture of the cellular motor is not complete since it does not contain the 1 min periodicity also observed.

Material transport is necessary for constructing the amoeboid cellular motor; new material must come to the plasma membrane and used material be taken away. In principle, the necessary molecules consumed in the signal chain could come to the plasma membrane by diffusion, but a transport system would be more efficient. Material flow can be observed in granulocytes migrating in a narrow glass tube. In the centre of the cell body, material is streaming towards the transparent amoeboid cellular motor; back streaming is close to the membrane at the glass wall. Microtubules are the classical transport system of cells. We suppose that the asymmetric distribution of the first and second intracellular messenger molecules causes orientation of the microtubules. On the other hand, the oriented cellular transport system (microtubules) can stabilize the asymmetric distribution of the first and second intracellular messenger molecules; thus, one expects a sharpening of their spatial distribution.

The cellular transport system can be disturbed by treating the cells with colchicine. One expects that the spatial mode of the instability in the signal chain is lowered for colchicine treated cells, e.g. granulocytes in the polar activated state ($n = 1$ mode) transform under the influence of colchicine to the isotropic activated state ($n = 0$ mode). A similar observation is made with melanocytes ($n = 2$ mode). If melanocytes are treated with colchicine then the large extended dendrites disappear and one observes the cells in the $n = 0$ mode.

5.7. *Different chemokinetic cellular machines*

The instability of the cellular signal chain has been discussed and verified for different cell types. Now we are interested in the machine properties of the spatial–temporal pattern. The model predicts different cellular machines based on a single chemical signal chain.

5.7.1. *Isotropic mode*

An inactivated cell without a leading front is usually not bound to the substrate, but the activated cell with its leading front is usually adherently bound. One can say that one basic function of the isotropic mode is adherence. The isotropic activated cellular mode makes an isotropically distributed leading front which produces a net force in the direction of the normal to the plane. The mean force parallel to the plane is zero as actually observed, but there are fluctuations in the signal chain which alter locally the force produced. These fluctuating forces are the cause of the appearance of a dynamically active leading front.

5.7.2. *Polar mode*

The model predicts a polar distribution of the first and second intracellular signal. The leading front points in one direction—the direction of migration. Two types of machine are realized by using only a single chemical signal chain. (i) Monopole machine (=steerer): the monopole of the distribution of the first intracellular signal molecules is used to produce the cellular speed. (ii) Dipole machine (=automatic controller): the dipole of the distribution of the first intracellular signal molecules with respect to a given direction is used to correct the angle of migration.

5.7.2.1. *Monopole machine.* The model predicts that the number of muscle proteins is proportional to the total amount of loaded receptors. Thus, one expects that the cellular speed is proportional to the fraction of loaded receptors.

$$v \propto \frac{c}{c + K_r}. \tag{21}$$

This prediction is verified by the experiments [9].

5.7.2.2. *Dipole machine*. The model predicts that the orientation of the leading front can be influenced by a weak external signal. The system actually acts as an automatic controller where the dipole moment of the distribution of the loaded receptors with respect to the direction of the guiding signal is used as a feedback signal. The chemical motor is rebuilt in such a way that the deviation angle, φ, will be diminished as expected for an automatic controller. The cellular device acts as a proportional controller since, for small angles ($\sin\varphi \approx \varphi$), the cellular reaction is proportional to the deviation between desired and actual angle.

The dipole machine can be characterized by the rate equation for the angle of migration

$$\frac{\mathrm{d}\varphi}{\mathrm{d}t} = -k_{\mathrm{P}} c_1(\text{field}) \sin\varphi + \Gamma_{\varphi}(t). \qquad (22)$$

The spatial pattern of the dipole machine is influenced by two contributions. (i) The first term describes the deterministic part of the automatic controller, where k_{P} is a signal transduction coefficient. $c_1(\text{field}) \sin\varphi$ originates from the dipole moment of the distribution of the loaded receptors with respect to the direction of the guiding signal. (ii) The second term describes stochastic processes in the dissipative structure. It is assumed that the largest contribution originates from the detection unit (vesicle fusion process). The angular distribution function, $f(\varphi)$, can be calculated if the stochastic processes are approximated by white noise; $\langle \Gamma_{\varphi}(t) \rangle = 0$ and $\langle \Gamma_{\varphi}(t) \Gamma_{\varphi}(t') \rangle = q_{\varphi} \delta(t - t')$. The steady state angle distribution function is obtained from the corresponding Fokker–Planck equation [18]

$$f(\varphi) = f_0 \exp\left(\frac{2 k_{\mathrm{P}} c_1}{q_{\varphi}} \cos\varphi \right). \qquad (23)$$

The proposed $\sin\varphi$ term is actually verified for different cell types and different guiding fields such as concentration gradient and electric field [19, 20]. The strength of the guiding signal influences directly the strength of the cellular reaction.

The cellular standard for an extracellular guiding signal is given by $2k_{\mathrm{P}} c_1 / q_{\varphi} = 1$, where the deterministic part of the first intracellular signal equals the stochastic part, i.e. the mean dipole moment of the first or second messenger distribution equals the strength of the dipole moment fluctuations. The taxis coefficient $2k_{\mathrm{P}}/q_{\varphi}$ describes the sensitivity of the cellular automatic controller; it can be determined by measuring the cellular response at different guiding field strengths. The quantification of random walk yields the fluctuation in the signal chain; they are quantified in case of the $n = 1$ mode by q_{φ}. One finds for granulocytes $2/q_{\varphi} = 60$ s [18]. The calculated temperature required is 4×10^4 K if the random walk were produced by thermal motion; this number demonstrates that the motion of the granulocyte is completely determined by active processes.

The asymmetric spatial distribution of the loaded receptors is the essential signal in the dipole machine. In the case of chemotaxis it is the asymmetric loading of the receptors, and in the case of galvanotaxis it is the asymmetric supply of membrane-bound receptors.

Chemotaxis. In the case of a concentration gradient of chemokinetic molecules, the dipole moment of the distribution of the first intracellular signal can be estimated by comparing the loaded receptors on the left side with those on the right side. One obtains for an oblique leading front with respect to the concentration gradient

$$\frac{c K_{\mathrm{R}}}{(c + K_{\mathrm{R}})^2} \frac{\mathrm{d}c}{c\,\mathrm{d}x} \sin\varphi. \qquad (24)$$

This prediction is verified for granulocytes and also for other cell types like single slime mould cells.

Galvanotaxis. Directed migration is obtained if cells are exposed to an electric field in an isotropic chemical environment. The proposed mechanism is that the vesicle fusion process can be influenced by an externally applied electric field. One obtains for an oblique leading front an additional voltage drop across the leading front $\propto E \sin\varphi$, since the intracellular space has a uniform electric potential due to the high resistivity of the membrane. This prediction is actually verified for many cell types like granulocytes, fibroblasts, neural crest cells, etc. [18].

The directed migration can be summarized in a dose–response curve; the dose is the strength of the extracellular guiding signal. The cellular response is the average of $\cos\varphi$—the polar order parameter. A universal representation is obtained if the extracellular guiding signal is measured in cell-made units; one obtains this dimensionless guiding signal from the angle distribution function. The dose–response curve is a universal curve as long as the automatic controller has the following properties: the cellular response is proportional to (i) $\sin\varphi$ and to (ii) the strength of the guiding field. The theoretical prediction, as well as the actual measurements are shown in figure 9; this holds true for different cell types such as granulocytes, monocytes, osteoblasts, fibroblasts, neural crest cells, etc. and for different guiding signals like concentration gradient and electric field. The model is not restricted to migrating cells—it also holds true for growing cells like hyphen (roots) of neurospora crassa.

Summarizing this part. (1) Cells have a steerer for the speed; the monopole of the first intracellular signal distribution acts as gas pedal. (2) Cells have an automatic

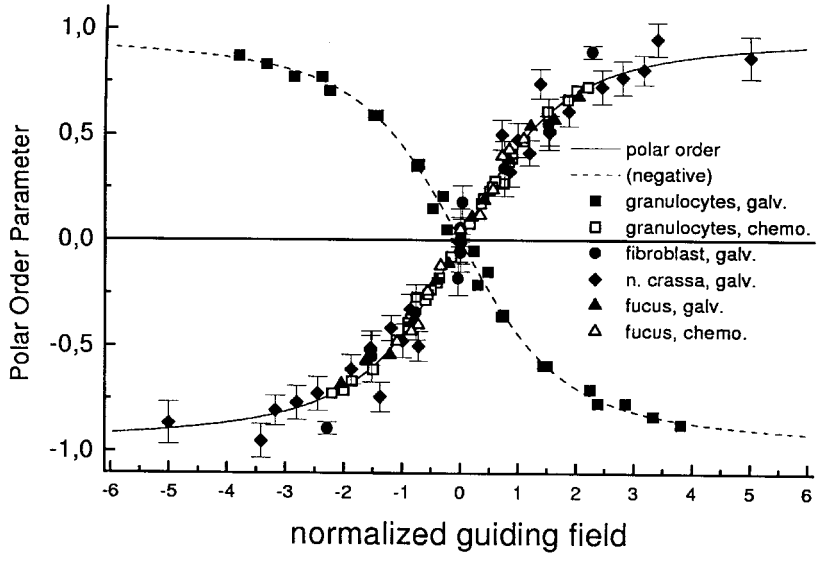

Figure 9. The steady state polar dose–response curve is shown for different cells and different guiding signals. The solid line is a prediction.

controller for the angle of migration; the dipole of the first intracellular signal distribution acts as steering wheel.

5.7.3. *Bipolar mode*

5.7.3.1. *Quadrupole machine*. A cell in a bipolar mode can have different kinds of machine: (i) a steerer for the speed of migration, (ii) an automatic controller for the angle of migration and (iii) an automatic controller for the angle of orientation. The model predicts that the orientation of two opposing motors can be influenced by a weak external signal. The system actually acts as an automatic controller where the quadrupole moment of the distribution of the loaded receptors with respect to the direction of the guiding signal is used as a feedback signal. The chemical motors are rebuilt in such a way that the deviation angle, ψ, will be diminished as expected for an automatic controller. The cellular device acts as a proportional controller, since for small angles ($\sin 2_\psi \approx_\psi$) the cellular reaction is proportional to the deviation between desired and actual angle.

The rate equation of the angle of orientation is [19]

$$\frac{\mathrm{d}\psi}{\mathrm{d}t} = -k_2 c_2 \sin 2\psi + \Gamma_\psi(t). \qquad (25)$$

The first term describes the deterministic part of the signal chain as described above and the second term the stochastic processes. Again it is assumed that the largest contribution originates from the detection unit (vesicle fusion process). The angle distribution function, $f(\psi)$, can be calculated if the stochastic processes are approximated by white noise ($\langle \Gamma_\psi(t) \rangle = 0$ and $\langle \Gamma_\psi(t)\Gamma_\psi(t') \rangle = q_\psi \delta(t - t')$). The predicted steady state angle distribution function is

$$f(\psi) = f_0 \exp\left(\frac{2k_2 c_2}{q_\psi} \cos 2_\psi\right). \qquad (26)$$

The proposed $\sin 2\psi$ term is actually verified for different cell types and different guiding fields such as electric field, periodically stretched surface, bent surface [21]. The strength of the guiding signal influences the strength of the cellular reaction; a strong cellular reaction is expected for a strong guiding signal and a weak reaction for a weak signal.

The cell orientation can be summarized in a dose–response curve. The dose is the strength of the extracellular guiding signal; the cellular response is the average of $\cos 2\psi$—the apolar order parameter. A universal representation is obtained if the extracellular guiding signal is measured in cell made units; it is actually the deterministic part of the cellular signal chain divided by the stochastic one. One obtains this dimensionless guiding signal from the angle distribution function. The apolar dose–response curve is a universal curve as long as the automatic controller has the following properties: the cellular response is proportional to (i) $\sin 2\psi$ and to (ii) the strength of the guiding field as seen by the cell. Theoretical predictions as well as the actual measurements are shown in figure 10. This holds true for different cell types such as osteoblasts, fibroblasts, neural crest cells, etc. and for different guiding signals like an electric field, periodically stretched surface and bent surface. The model is not restricted to orienting cells; it also holds true for growing cells like hyphen (roots) of neurospora crassa.

It is interesting to see that a cell like a fibroblast has

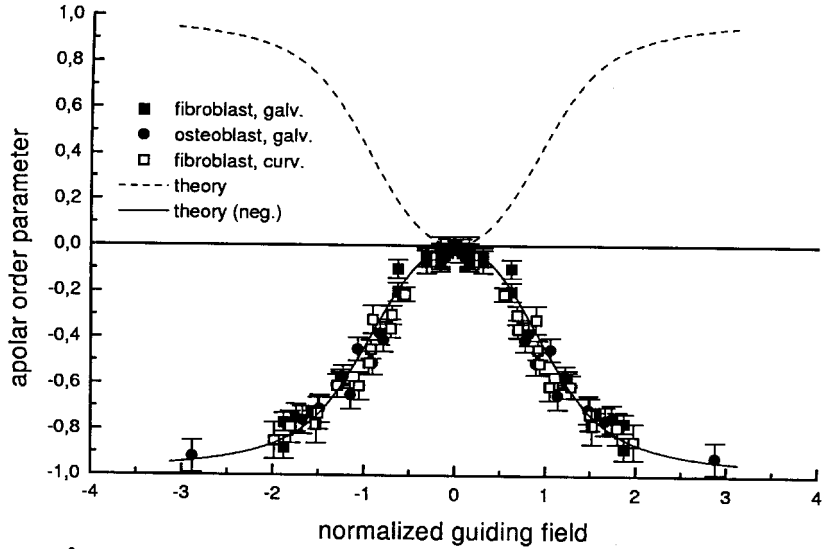

Figure 10. The steady state apolar dose–response curve is shown for different cells and different guiding signals. The solid line is a prediction.

a different reaction to an electric field. A fibroblast performs a directed migration towards the cathode. This cellular response is proportional to the electric field strength ($c_1 \propto E$) [18]. A further cellular response is the cell rotation. A fibroblast tries to orient its long axis perpendicular to the field; this cellular response is proportional to the square of the electric field ($c_2 \propto E^2$) [22]. This is an indirect proof that one has two independently working machines.

Summarizing this part. (1) Cells have a steerer for the speed; the monopole of the first intracellular signal distribution acts as a gas pedal. (2) Cells have an automatic controller for the angle of migration; the dipole of the first intracellular signal distribution acts as steering wheel. (3) Cells have an automatic controller for the orientation angle; the quadropole of the first intracellular signal distribution acts as steering wheel.

6. Living liquid crystals

Cells have the ability for active migration. Random walk is obtained in the case of no extracellular signal or one with isotropic distribution, but the movement or the orientation becomes directed or oriented if an extracellular guiding signal is applied. The previous experiments were performed at low cell density so that one cell is not influenced by other cells; now we will consider interacting cells without an applied extracellular guiding signal. A liquid crystal is expected if one arbitrary cell is guided by the submitted signal of all the other cells. Two types of living liquid crystals are discussed: (i) a polar nematic liquid crystal obtained when the interacting cells produce a polar guiding field which induces directed movement, and (ii) a classical nematic state for an apolar guiding field.

6.1. *Polar nematic liquid crystal*

The instability of the cellular signal chain is discussed in the framework of the vesicle fusion process as one basic step in the signal rectification process. The vesicle fusion process is the essential feedback element in the intracellular signal chain, but this process can also be used for extracellular signalling if the vesicles contain a chemoattractant. The released signal molecule of granulocytes at low calcium content is still not known, but it is c-AMP in the case of slaved slime mould cells. The single migrating cells start to form a cluster which is the initial step for building up in the third dimension fruit bodies bearing spores.

The cluster formation of migrating cells is discussed in the framework of a mean-field. The number of cells in one cluster is regarded as the order parameter which slaves the cells.

The attraction mechanism is based on (i) intrinsic properties of the cell and (ii) the extracellular guiding field which is produced by the other cells. The local cell density, n, can be altered by the cell–cell attraction and cell diffusion. In the case of many cells, it is difficult to sum up all the pair interactions and to predict the behaviour of these cells, therefore the interaction of *one* with all the *others* can be approximated by introducing a mean guiding field. Let us consider a cluster of densely packed, but migrating cells. The gain is the number of attracted cells per unit time. It should be proportional to the cell density, ρ, in the vicinity of the cluster and

to the number of cells, n, in a cluster (gain $= a_+ n\rho$). The cells can only leave the cluster at the boundary. The number of cells at the boundary is proportional to the square root of n (loss $= a_- n^{1/2}$). The rate equation for one cluster is

$$\frac{\partial n}{\partial t} = a_+ n\rho - a_- n^{1/2}. \tag{27}$$

In addition one has $\rho_0 = (Z/A)n + \rho$ due to the conservation of the number of cells in the area A; ρ_0 and Z describe the cell density at the start of the experiment and the number of clusters, respectively.

$$\frac{\partial n}{\partial t} = a_+ n\rho_0 - a_- n^{1/2} - a_+ \frac{Z}{A} n^2. \tag{28}$$

This mean-field approach is actually verified for migrating granulocytes exposed to low calcium concentration [23, 24]. The cluster formation was a function of the mean cell density, ρ_0. A threshold behaviour was observed: at low cell density ($\rho_0 < \rho_{th} = 150 - 300$ cells mm^{-2}) the migrating cells did not form clusters. Mainly single migrating cells were observed, but occasionally two or three cells stayed together for several minutes. At high cell density ($\rho_0 > \rho_{th}$), the migrating cells formed clusters with a very long lifetime (1–2 h). But the clusters were not stable; they dissolved themselves for large times $t > 1$–2 h.

The cluster formation could start with two granulocytes having direct contact of their leading fronts. At this contact the membrane of the leading front showed an enhanced fluctuation. It seemed that one granulocyte was attracted by the leading front of another one; these two 'kissing' cells attracted further cells which tried to get direct contact with the leading fronts of the 'kissing' cells. In large sized clusters, the cells were oriented towards the centre (figure 11). The polar order parameter, $\langle \cos \varphi \rangle$, was between 0·60 and 0·80; the cell orientation was singular at the centre of the cluster. The experiments were repeated with a small concentration of monocytes kept in the isotropic activated state. The monocytes adhere to the substrate and are surrounded by a leading front; they do not migrate. Nucleation starts preferentially at the spatially fixed monocytes but when the cluster is formed the monocyte is squeezed out and replaced by a granulocyte.

The cells in a cluster try to move towards the cluster's centre; but this movement is hindered, since the cluster is already densely packed with cells. Thus, the movement of one cell is successful if it can take the place of another cell which is squeezed out. The pressure and the force created by one stopped cell is ≈2000 Pa and 40 nN, respectively [25]. We have a situation where the cells are polar oriented, but the centre of mass is more or less statistically distributed. Hence, we have a state of a

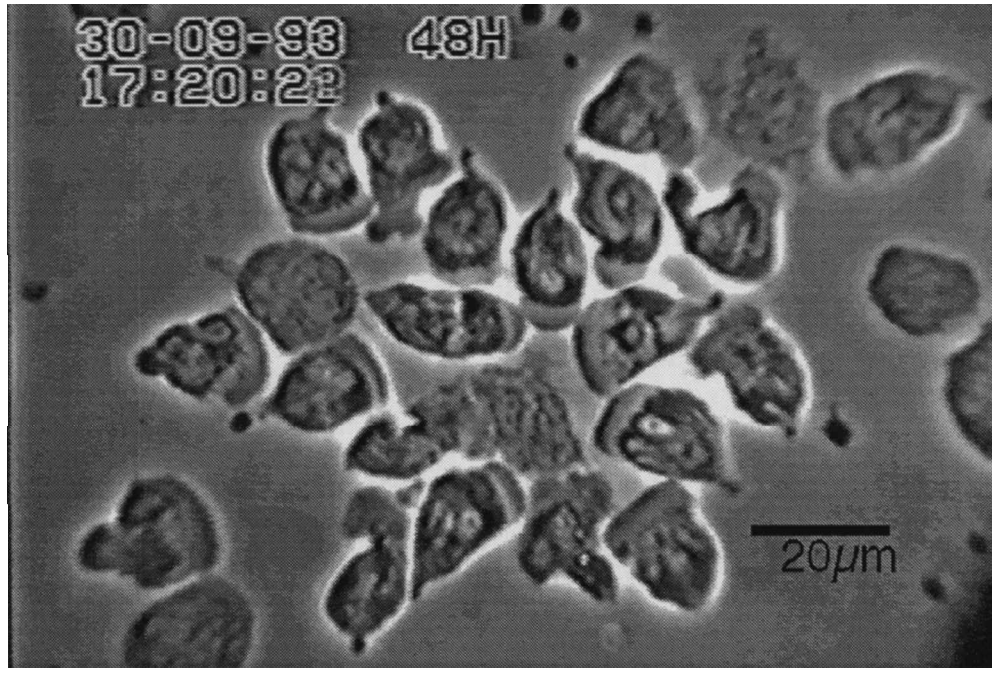

Figure 11. Granulocytes at low calcium concentration attract each other; clusters are formed at high enough cell densities. The cells try to move towards the centre; the centre is here a monocyte in the isotropic activated state (spherical shaped cell). The cells are oriented towards the centre of the cluster and form a polar nematic liquid crystal. Another monocyte is in the upper right side which is starting to attract granulocytes.

polar nematic liquid crystal: no order in the centre of gravity, but order in the orientation of the elongated elementary units.

6.2. *Apolar nematic liquid crystal*

Cells in the bipolar state tend to orient their long axes perpendicular to the extracellular guiding signal; one could say that the cells like to minimize the extracellular disturbance. With this knowledge in mind, one expects a nematic liquid crystal to attract cells having an elongated shape since the free volume is reduced if the cells orient their long axis in a preferred direction.

The machine equation for the orientation angle of a single cell is a stochastic equation as previously discussed, equation (25). The extracellular field will now be exchanged by a mean field which is produced by all the other cells. One expects that the mean field is proportional to the cell density, ρ, to the apolar order parameter, $\langle \cos 2\psi \rangle$. The coefficient c_2 in equation (25) is then

$$c_2 = \rho \langle \cos 2\psi \rangle a_2. \tag{29}$$

where a_2 calibrates the mean field. The rate equation for the angle distribution function (Fokker–Planck equation) is

$$\frac{\partial \psi}{\partial t} = \frac{\partial}{\partial t}\left(c_2 \sin 2\psi + \frac{q_\psi}{2}\frac{\partial}{\partial \psi} \right) f \tag{30}$$

if the stochastic processes are described by white noise [$\langle \Gamma_\psi(t) \rangle = 0$ and $\langle \Gamma_\psi(t)\Gamma_\psi(t') \rangle = q_\psi \delta(t - t')$]. The first term tries to create a sharp distribution where all the cells are oriented parallel to each other; the second term tries to create a homogeneous distribution where all orientation angles have the same probability. These two processes define the steady state angle distribution function. The apolar order parameter, as the average of $\cos 2\psi$, can be calculated if the angle distribution function [equation (26)] is known. One obtains

$$\langle \cos 2\psi \rangle = \int_0^{2\pi} \exp\left(\frac{2k_2 a_2}{q_\psi} \rho \langle \cos 2\psi \rangle \cos 2\psi \right) \cos 2\psi \, \mathrm{d}\psi. \tag{31}$$

It is a self-consistence relation for the existence of the nematic phase, since the calculated apolar order parameter (left side of this equation) has to be used in the mean field (right side of this equation). For low cell density, the stochastic process is stronger than the orienting process and the cells are randomly oriented as actually observed. But for high cell density the orienting process is stronger than the stochastic process and a nematic liquid crystalline phase is expected. One can say that the apolar order parameter slaves the single cells.

This mean-field approach is actually verified for melanocytes [26]. At low cell density ($\rho < \rho_{th} \approx 55$ cells mm^{-2}) the cells did not form a nematic liquid crystal and were randomly oriented. At high cell density ($\rho > \rho_{th}$), melanocytes formed a stable nematic liquid crystal (figure 12). The experiments were performed from days up to several weeks [27]. The apolar order parameter as a function of the cell density is quite well described by the mean-field theory where the threshold concentration is the only fitting parameter.

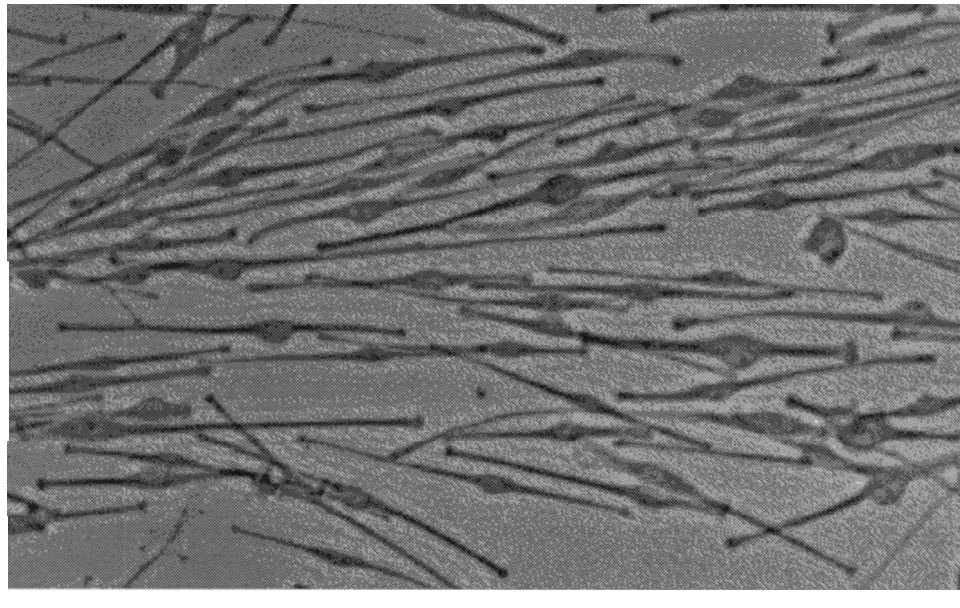

Figure 12. Melanocytes in the bipolar state on a glass surface are shown. The characteristic length of the cells is about 100 μm. The cell orientation is random at low cell density; the cells are oriented in one direction at higher cell densities. The cells form an apolar nematic liquid crystal.

An apolar nematic liquid crystal is formed by other cell types such as fibroblasts, osteoblasts, preadipocytes, etc.

7. Outlook

A common concept for understanding systems far from thermodynamic equilibrium has been applied to fluid systems. Interest was focused on fluid machines. Coherent processes which are needed in every type of machine are created by instabilities, therefore every instability which shows ordering phenomena should be investigated with respect to building new types of machine. It is the start of a new technology and therefore one should not be disappointed if the newly constructed machine has no application, as demonstrated with the fluid self-organized automobile.

Fluid self-organized machines represent a new and important field in the triangle between physics, chemistry and life sciences. It is important, e.g. in a cell, to know all steps of the biochemical reaction chain, but in addition, one has to find the processes which create the machine (coherence in the signal chain). Knowledge of the biochemical events and of the details of the working machine could lead to new frontiers. For example, phenomena in cell biology are usually discussed on a molecular basis; the new concept is to discuss such phenomena additionally on the basis of self-organized machines. This means, in the case of pharmacology, that compound design should not neglect the machine aspects.

The processes by which particles such as molecules or living cells exchange information constitute one of the most intriguing areas of physics and life sciences. The physical process of reducing a gas containing free molecules to a liquid form, or an isotropic liquid to a liquid crystal, is understood to a large extent, and the mean behaviour of a given molecule in the interaction field of the other moving molecules may be determined by Boltzmann statistics. Surprisingly, identical principles are used to reduce freely migrating cells to a condensed state. The self-organization of fluid systems to ordered structures plays an important role in morphogenesis, organogenesis, wound-healing, etc. Here it is important to realize that the self-organized cellular system is much more sensitive to extracellular signals than the single cell. This knowledge opens up new therapeutic possibilities.

This work was supported by Deutsche Forschungsgemeinschaft, Fond der Chemischen Industrie, Fondation de France and INSERM U313. The author thanks M. Eberhardt and R. Kemkemer for stimulating discussions and A. Chevance de Bois-Fleury (Paris) and D. Kaufmann (Ulm) for their encouragement and help in cell biology.

References

[1] Haken, H., 1983, *Synergetics* (Heidelberg, Berlin: Springer).
[2] Schenkman, J. B., and Grein, H. (editors), 1993, *Cytochrom P 450* (Heidelberg, Berlin: Springer).
[3] Dupeyrat, M., and Nakache, E., 1978, *Bioelectr. Bioenerg.*, **5,** 134.
[4] Nakache, E., and Dupeyrat, M., 1983, *J. Colloid Interface Sci.*, **94,** 187.
[5] Gruler, H., Vilanove, R., and Rondelez, F., 1980, *Phys. Rev. Lett.*, **44,** 590.
[6] Hallett, M. B., 1989, *The Neutrophile: Cellular Biochemistry and Physiology*, 1989 (Boca Raton, Florida: CRC Press).
[7] Keller, H.-U., and Bessis, M., 1975, *Nouv. Rev. Fr. Hematol.*, **15,** 439.
[8] Malawista, S. E., and de Boisfleury-Chevance, A., 1982, *J. Cell Biol.*, **95,** 960.
[9] Schienbein, M., and Gruler, H., 1995, *Phys. Rev. E*, **52,** 4183.
[10] Franke, K., and Gruler, H., 1990, *Eur. Biophys. J.*, **18,** 335.
[11] Franke, K., and Gruler, H., 1994, *Z. Naturforsch.*, **C49,** 241.
[12] Gerisch, G., and Keller, H.-U., 1981, *J. Cell Sci.,* **52,** 1.
[13] Jäger, U., Gruler, H., and Bültmann, B. D., 1988, *Klin. Wochenschr.*, **66,** 434.
[14] Weis, S., 1994, Diplomarbeit, Universität Ulm.
[15] Dyett, D. E., Malawista, S. E. Naccache, P. H., and Sha'afi, R. I., 1986, *J. Clin. Invest.*, **77,** 34.
[16] Wymann, M. P., Kernen, P., Bengtsson, T., Baggiolini, M., and Derauleau, D. A., 1990, *J. Biol. Chem.*, **67,** 2535.
[17] Franke, K., and Gruler, H., 1994, *Z. Naturforsch.*, **C49,** 241.
[18] Schienbein, M., Franke, K., and Gruler, H., 1994, *Phys. Rev. E*, **49,** 5462.
[19] Gruler, H., 1991, in *Biologically Inspired Physics*, edited by L. Peliti (New York: Plenum Press), pp. 217–227.
[20] Gruler, H., 1990, in *Lecture Notes in Biomathematics: Biological Motion*, edited by W. Alt and G. Hoffmann (Berlin, Heidelberg: Springer), pp. 396–414.
[21] Kemkemer, R., Neidlinger-Wilke, C., Claes, L., and Gruler, H., *Cell Biochem. Biophys.* (in press).
[22] Erickson, C. A., and Nuccitelli, R., 1984, *J. Cell Biol.*, **98,** 296.
[23] Gruler, H., and de Boisfleury-Chevance, A., 1994, *J. Phys. I Fr.,* **4,** 1085.
[24] Gruler, H., Schienbein, M., Franke, K., and de Boisfleury-Chevance, A., 1995, *Mol. Cryst. Liq. Cryst.*, **260,** 565.
[25] Vereycken, V., Gruler, H., Bucherer, C., Lacombe, C., and Lelièvre, J. C., 1995, *J. Phys. III Fr.*, **5,** 1469.
[26] Gruler, H., Dewald, U., and Eberhardt, M. (to be published).
[27] Dewald, U., 1996, Diplomarbeit, Universität Ulm.